Broadband supercontinuum generation at the ultraviolet and visible wavelengths based on the higher-order modes of hollow-core photonic crystal fiber

DAGUI WANG[a,*], XIANGWEI SHEN[a], ZHONGCHAO WU[a], XIAOXIN WANG[a], JINHUI YUAN[b], XIAOLIANG HE[a], CHONGXIU YU[b]
[a]*26th Institute of China Electronics Technology Corporation, 400060, Chongqing, China*
[b]*State Key Laboratory of Information Photonics and Optical Communications Beijing University of Posts and Telecommunications 100876, Beijing , China*

Using the hollow-core photonic crystal fiber (HC-PCF) with the zero dispersion wavelengths of fundamental mode and second-order mode around 887 nm and 758 nm designed and fabricated in our lab, broadband supercontinuums (SC) from 180 nm to 1100 nm are efficiently generated in the ultraviolet and visible wavelengths by Ti: sapphire laser with working wavelength of 790 nm and pulse width of 120 fs. The influence of pump power on SC is also analyzed. The power ratio of the SC signal to the residual pump is calculated as 65:1, and the maximum conversion efficiency of 37% in the experiment is achieved.

(Received June 12, 2016; accepted November 28, 2017)

Keywords: Supercontinuum generation, Higher-order modes, Ultraviolet and visible wavelengths, Hollow-core photonic crystal fiber

1. Introduction

Supercontinuum generation (SCG) in hollow-core photonic crystal fibre (HC-PCF)[1-5] is a complicated nonlinear optical phenomenon characterized by a dramatic white light spectrum. Self-phase modulation (SPM), four-wave mixing (FWM), Raman self-frequency shift (RSFS), and paradigm of effective three-wave mixing (ETWM) are the main effects leading to the generation of a broadband spectrum in nonlinear PCFs [6-9]. The location between the pump wavelength and the zero-dispersion wavelength of the fundamental, second-order and third-order mode plays important role in SC generation. During the past decade, the mode characteristics including the guided modes and cladding modes lying in or beyond the photonic band gaps (PBGs) have been theoretically and experimentally investigated. During the past decade, several experiments and numerical simulations have been performed to investigate the dynamics of SC generation through exciting different order modes in normal and anomalous regimes [10-13].

Hou J. et al. design a seven-core photonic crystal fiber with specifically designed dispersion and group velocity profile which is optimized for high-power visible SC generation pumped by 1-μm pulsed lasers, and achieved a high-power SC extending to 400 nm by simulation , but not achieved by experiment [1]. Saini T S et al. generated SC spectra spanning 1480 - 9990 nm using only 4 mm length of proposed photonic crystal fiber pumped with femtosecond optical pulses of peak power of 500 W at 2800 nm. however, not cover ultraviolet [14]. Wadsworth et al. reported SC generation with Q-switched pulses in endlessly single-mode PCFs [15]. Yuan JH et al experimentally achieved Broad and ultra-flattened SC 400-800 nm based on the fundamental mode of photonic crystal fiber with central holes, however, not cover ultraviolet.

In this paper, 920 nm SC are efficiently generated from 180 nm to 1100 nm based on the higher-order modes of Hollow-Core Photonic Crystal Fiber. The power ratio of the SC signal to the residual pump is calculated as 65:1and the maximum conversion efficiency of 37% in the experiment is achieved.

2. The PCF properties and experiment

Beam propagation method (BPM) [16] has been used to analyze the properties of group velocity dispersion D of the irregular point of HC-PCF. Fig. 1 is the group velocity dispersion D, where $= -(2\pi c)/(\lambda^2)\beta^2$, $\beta^2 = \partial^2\beta(\omega)/\partial\omega^2$ and $_{\beta(\omega)}$ is the fiber mode-propagation constant, is calculated as a function of

wavelength for the fundamental mode of the irregular point of HC-PCF with zero dispersion wavelength the fundamental mode and third-order mode located at 887nm and 758 nm, respectively. The cross-section structure of HC-PCF is shown in inset 1 of Fig. 1, where the average cladding air hole diameter d=2.6 μm, hole to hole pitch Λ=3.1μm, the average core diameter D=2.7 μm, and the air filling fraction f=0.8.

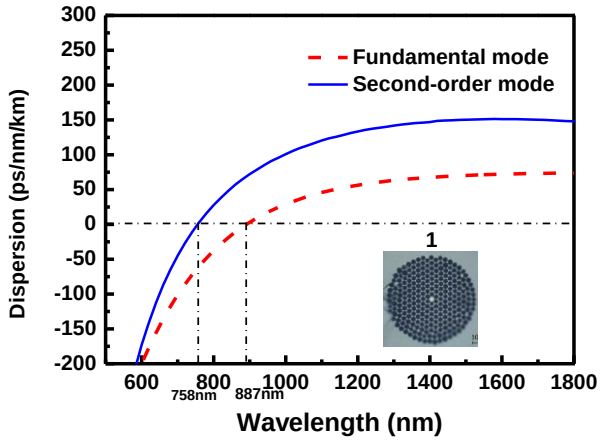

Fig. 1. Group-velocity dispersion calculated as a function of radiation wavelength for the fundamental mode and second-order mode are located at 887 nm and 758 nm, respectively. The insert 1 show the whole cross-section of HC-PCF used in experiment

The configuration of experimental setup is given in Fig. 2. The light source was a mode-locked Ti:sapphire laser, emitting a pulse train with full width at half maximum (FWHM) of 120 fs at the repetition rate of 76 MHz. A variable attenuator is placed behind the laser to control the input energy and isolator is inserted to block the back-reflection from the input tip of the fiber into the laser cavity. The 40× objective lens with numerical aperture of 0.8 are used for adjusting input and output efficiency. CCD1 and CCD2 are used to observe the output mode field and check the coupling state of input field respectively. With the offset pumping technique, the light energy is mainly coupled into the second-order mode. The beam goes through the first split-beam mirror, one part is coupled into power meter to monitor the input average power, and the other part is coupled into the HC-PCF span of 1 m length. The coupling efficiency is above 70%. The transmission loss is 8 dB/m at 810 nm with the cutback method. The output spectra are monitored by optical spectrum analyzer (OSA, Avaspec-256) with the measurement scopes from 200 to 1100 nm and the resolutions of 0.025 nm.

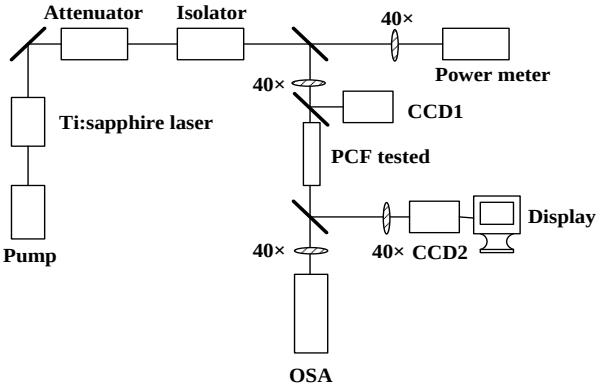

Fig. 2. The configuration of experimental set-up

3. Results and discussion

The experiment is carried out by coupling fs pulse with working wavelength of 790 nm (lying in the anomalous dispersion region of the second-order mode) and average power from 550 mW to 750 mW into the HC-PCF. The second-order mode are excited selectively to achieve phase-matching FWM.

As shown in Fig. 3(a), while the input pump is at the anomalous dispersion region of 790 nm and the average power of 750 mW is mainly coupled into the second-order mode, the remarkable broadband SC is generated from 180 nm to 1100 nm. The ultra-violet part of SC can below 180 nm and at the same time the mid-infrared part of SC is generated, which limited by the measurement range of OSA. The area ratio of the SC and the residual pump is chose to calculating the ratio of the SC signal to the residual pump. With the input average power increasing from 550 mW to 750 mw, the power ratio of the SC signal to the residual pump can up to 65:1. The observed output far field modes at different signal wavelengths (orange-yellow, green-white, and yellow-white) are shown in Fig. 3(b). The different color of the experiment HC-PCF (green, purple, and pink) are shown in Fig. 3(c).The conversion efficiency (η) of the degenerate FWM can be described by the power ratio of the output SC signal and incident pump. For the determinate coupling efficiency (65%), with the input average power increasing from 550 mW to 750 mw, the maximal η in the experiment is estimated as 37%.

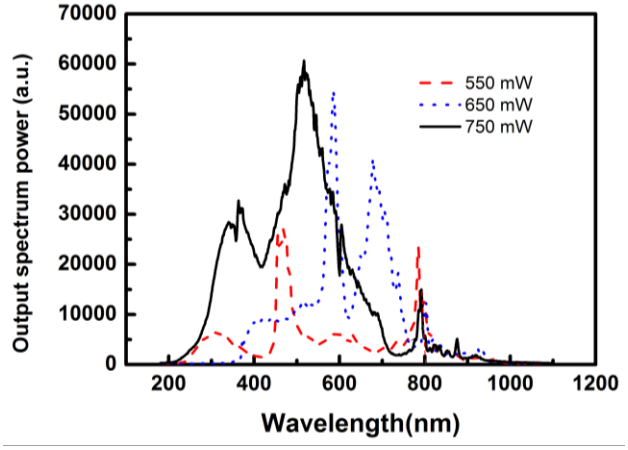

(a)

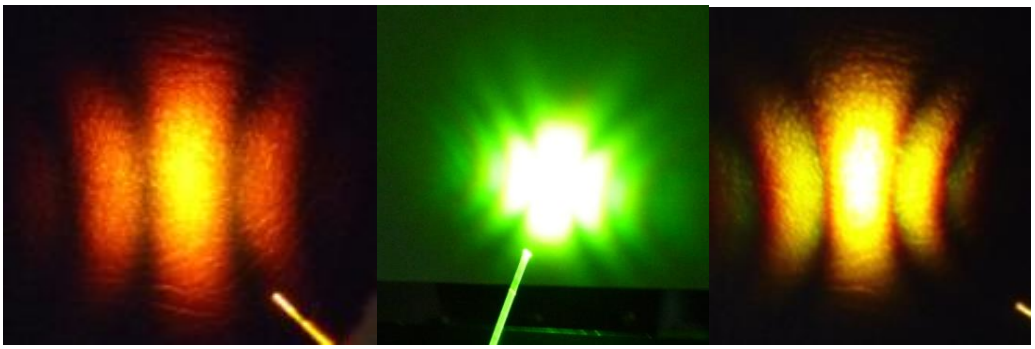

(b)

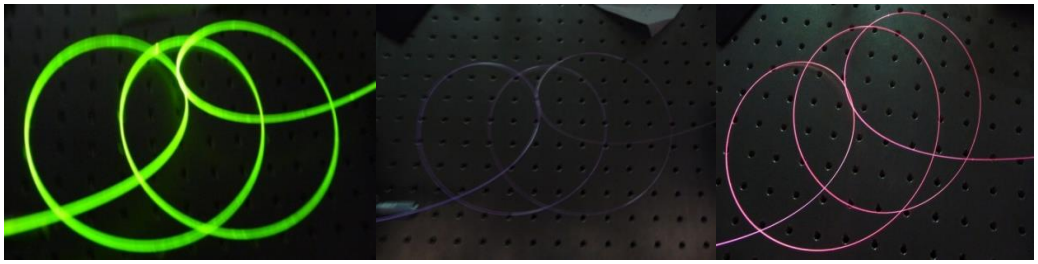

(c)

Fig. 3. When the pump with working wavelength of 790 nm and the input average power increases from 400 to 600 mW, (a) the output spectra increase from 100 to 1200 nm,(b) The corresponding far filed observed at different wavelengths (orange-yellow, green-white, and yellow-white), (c) The different color of the experiment HC-PCF (green, purple, and pink)

4. Conclusions

920 nm SC based on the second-order mode of PCF are efficiently generated by coupling a train of femtosecond pulses into HC-PCF. When the pump power increase from 400 to 600 mW, the ultra-violet part of SC is below 180 nm and the power ratio of the SC signal to the residual pump can up to 65:1.

Acknowledgments

This work is partly supported by the National Key Basic Research Special Foundation (2010CB327605 and 2010CB328300), and the Fundamental Research Funds for the Central Universities under (2011RC0309 and 2011RC008), and the Specialized Research Fund for the Doctoral Program of Beijing University of Posts and Telecommunications (CX201023).

References

[1] J. Hou, Opt. Express **54**(6), 066102 (2015).
[2] P. Jamatia, T. S. Saini, A. Kumar, R. K. Sinha, Appl. Opt. **55**(24), 6775 (2016).
[3] U. D. Dave, S. Uvin, B. Kuyken, et al., Opt. Express **21**(26), 32032 (2013).
[4] K. M. Ho, C. T. Chan, C. M. Soukoulis, Phys. Rev. Lett. **65**(25), 3125 (1990).
[5] J. H. Yuan, X. Z. Sang, C. X. Yu, et al., Chinese Physics B **20**, 054210-1-6 (2011).
[6] J. C. Knight, Nature **424**, 847 (2003).
[7] X. Jiang, N. Y. Joly, M. A. Finger, Opt. Lett. **41**(18), 4245 (2016).
[8] J. H. Yuan, X. Z. Sang, C. X. Yu, et al., Chin. Phys. B **19**, 074218 (2010).
[9] J. H. Yuan, X. Z. Sang, C. X. Yu, et al., IEEE J. Quantum Electron. **46**(5), 728 (2010).
[10] J. H. Yuan, X. Z. Sang, C. X. Yu, et al., J. Lightwave Technol. **29**(19), 2920 (2011).
[11] J. M. Dudley, L. Provino, N. Grossard, et al., J. Opt. Soc. Am. B **19**(4), 765 (2002).
[12] A. Gaeta, Opt. Lett. **27**(11), 924 (2002).
[13] I. Cristiani, R. Tediosi, L. Tartara, et al., Opt. Express **12**, 4366 (2004).
[14] T. S. Saini, A. Baili, A. Kumar, et al., Journal of Modern Optics **62**(19), 1570 (2015).
[15] W. Wadsworth, N. Joly, J. C. Knight, et al., Opt. Express **12**(2), 299 (2004).
[16] G. R. Hadley, J. Lightwave Technol. **16**(1), 134 (1998).

*Corresponding author: wdgsxw@163.com